crystals

MDPI

Article

Ab Initio Investigation of the Mechanics and Thermodynamics of the Cubic $EuAlO_3$ and $GdAlO_3$ Perovskites for Optoelectronic Applications

Adel Bandar Alruqi [1,*] and Nicholas O. Ongwen [2]

[1] Department of Physics, Faculty of Science, King Abdulaziz University, Jeddah 21589, Saudi Arabia
[2] Faculty of Biological and Physical Sciences, Tom Mboya University, Homa Bay 40300, Kenya
* Correspondence: aalruqi@kau.edu.sa

Abstract: Perovskites are currently becoming common in the field of optoelectronics, owing to their promising properties such as electrical, optical, thermoelectric, and electronic. Although mechanical and thermal properties also play a crucial part in the functioning of the optoelectronic devices, they have scarcely been explored. The present work performed an ab initio study of the mechanical and thermal properties of the cubic $EuAlO_3$ and $GdAlO_3$ perovskites for the first time using density functional theory. *Quantum Espresso* and *Themo_pw* codes were utilized by employing the generalized gradient approximation. Although the results showed that both materials have good mechanical and thermal properties that are ideal for the above–mentioned applications, $EuAlO_3$ possessed better structural and thermal stability, bulk modulus, Poisson ratio, thermal expansion coefficient, and thermal stress; while $GdAlO_3$ possessed better Young's modulus and shear modulus. Moreover, the mechanical properties of the two materials turned out to be much better than those of the common materials for optoelectronic applications, while their thermal properties were comparable to that of sapphire glass. Since this study was computational, an experimental verification of the computed properties of the two materials needs to be carried out before they can be commercialized.

Keywords: perovskite materials; temperature–dependent elastic constants; thermal expansion coefficients of $EuAlO_3$ and $GdAlO_3$; thermal stress of $EuAlO_3$ and $GdAlO_3$; ductility of $EuAlO_3$ and $GdAlO_3$; materials for optoelectronic applications

check for updates

Citation: Alruqi, A.B.; Ongwen, N.O. Ab Initio Investigation of the Mechanics and Thermodynamics of the Cubic $EuAlO_3$ and $GdAlO_3$ Perovskites for Optoelectronic Applications. *Crystals* **2024**, *14*, 1084. https://doi.org/10.3390/cryst14121084

Academic Editor: Xiaoping Wang

Received: 8 November 2024
Revised: 23 November 2024
Accepted: 26 November 2024
Published: 16 December 2024

Copyright: © 2024 by the authors. Licensee MDPI, Basel, Switzerland. This article is an open access article distributed under the terms and conditions of the Creative Commons Attribution (CC BY) license (https://creativecommons.org/licenses/by/4.0/).

1. Introduction

Perovskites are a class of materials with a particular crystal structure, with the chemical formula ABX_3 (here, "X" stands for an anion, and "A" and "B" for cations); and have an overall structure composed of a cubic arrangement of anions, in which the cations occupy particular lattice points [1]. The properties of perovskite materials and their prospective applications in several industries, including solar cells, are wide ranging and have generated a lot of interest. Their electrical, electronic, optical, and magnetic properties all work together to enable photovoltaic applications, which have shown great promise due to their high efficiency, low manufacturing costs, and potential for flexible and lightweight devices [2,3].

Perovskite–based light emitting diodes (LEDs) are attractive possibilities for next–generation lighting systems due to their high sensitivity to environmental changes, high efficiency, and color purity. They can be used in sensors that identify gases, liquids, and other compounds because of their properties, in addition to being useful in chemical reactions that produce fuels or other important molecules (as a number of these perovskite materials have shown catalytic activity) [4]. Current research has focused on materials that can be used as dielectrics and substrates for high temperature superconducting microwave devices, of which rare earth aluminate ($RAlO_3$) perovskites (where R stands for La, Ce, Pr, Nd, Pm, Sm, Eu, and Gd) are widely employed in the epitaxy of a variety of materials [5];,with the tolerance factor linked to crystal symmetry playing a crucial role in

imparting a material's dielectric properties [6]. $XAlO_3$ (Sm, Gd, and Eu) has been shown to exhibit a perovskite structure in the orthorhombic phase, as well as the rhombohedral phase [7], where its dielectric properties are studied by various groups too. The lanthanides are also used in applications such as solid oxide fuel cells, active and passive laser media [8], and scintillators [9].

Previous studies on $EuAlO_3$ have shown that it is a wide–bandgap insulator (band gap of 4–5 eV) under standard conditions. Its electrical resistivity is high, which makes it a good dielectric material. Moreover, it exhibits notable dielectric permittivity, often influenced by temperature and applied frequency, in addition to exhibiting ionic conductivity due to oxygen vacancies, especially when doped with aliovalent cations. The luminescence due to Eu^{3+} ions make $EuAlO_3$ a candidate for optoelectronic applications [10,11]. Studies have shown that $GdAlO_3$ is also a wide–bandgap insulator (band gap of 2.9–5 eV). Its high electrical resistivity makes it suitable for dielectric and insulating applications [12].

A recent study explored the cubic phase of $XAlO_3$ (X = Sm, Eu, and Gd) materials in terms of their electrical, optical, and thermoelectric behavior via spin polarization for potential utilization in opto/energy applications [7], and reported that the materials exhibit interesting properties for the aforementioned applications. However, although their electrical and optoelectronic properties (providing useful information for solar cells) have been explored using various methods, their mechanical/thermal properties, which are also crucial in order to fully describe their performance in optoelectronic devices such as dye-sensitized solar cells, are yet to be comprehensively studied. While the heat capacity of $EuAlO_3$ and their mechanical properties have been explored [13,14], their thermal properties have not been investigated. For the first time, this work reports a detailed study of mechanical and thermodynamic properties of $EuAlO_3$ and $GdAlO_3$ perovskites. The study aimed to compare the mechanical and thermal properties of the two materials in order to describe their choice for developing optoelectronic devices.

2. Materials and Methods

The crystallographic information files used for the calculations of $EuAlO_3$ and $GdAlO_3$ were obtained from materials project website [15,16]. The unit cells were cubic, with space group $Fm\bar{3}m$, and lattice constants of a = 3.768Å and a = 3.735Å for $EuAlO_3$ and $GdAlO_3$, respectively. Figure 1 shows the 3D structures of the two cells. The optimization of the kinetic energy cut–off (ecut) was done by varying it from 20 to 90 Ry in steps of 10 Ry, while the optimization of the k–points was done by varying it from 2 2 2 to 9 9 9 in steps of 1 1 1. Furthermore, the optimization of the lattice parameters and the lattice points on the cells were done by performing variable cell relaxation, by setting the optimized ecut at 50 Ry (the point at which the curve of total energy against ecut flattened), the optimized charge density at 400 Ry, and the optimized k-points at 5 5 5 (the point at which the curve of total energy against k–point flattened). Although setting higher values of the ecut and k–points would have improved the accuracy of the results, higher values are computationally expensive (which is one of the limitations of density functional theory (DFT) that was employed in this study). Moreover, at the above settings, the total energy difference was 4.2×10^{-4} Ry and 3.1×10^{-4} Ry respectively for ecut and k–points. Optimization of the lattice points was done using the Broyden–Fletcher–Goldfarb–Shanno algorithm. Ultrasoft pseudopotentials by Perdew–Burke–Ernzerhof were utilized within the generalized gradient approximation, which was chosen over the local density approximation, which highly underestimate the lattice parameters and overestimate the mechanical properties. We made use of the *Quantum Espresso* package [17].

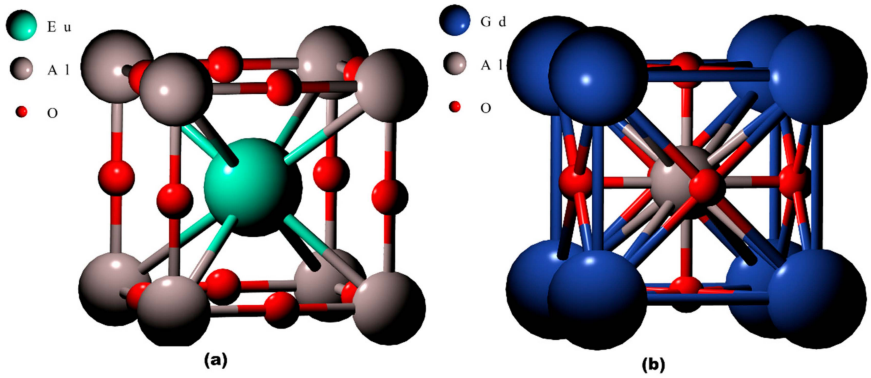


Figure 1. The 3D structures of **(a)** $EuAlO_3$ and **(b)** $GdAlO_3$.

In order to test the structural stabilities of the two materials, their formation energies were calculated according to the relation [18]:

$$H_f^{XAlO_3} = E(XAlO_3) - \lambda_X - \lambda_{Al} - 3\lambda_O, \quad (1)$$

with X = EuorGd, and $\lambda_X, \lambda_{Al}, 3\lambda_O$ are the total energies of the individual atoms. The mechanical properties calculation was performed by following the work from a previous study [19] using small strains within ± 0.005, so as to remain within the linear regime of the crystals, both at the ground state and as functions of temperature. The thermal properties calculation was made possible thanks to the *Thermo_pw code* [20]. For the calculations, the temperature range (233–358 K) was selected in line with the operational ranges for various optoelectronic devices such as photodetectors, semiconductor LEDs, and laser diodes. The phonon threshold was fixed at 1×10^{-12}, while nq_1, nq_2, and nq_3 were fixed at 5 (the same value as for the k–point mesh).

3. Results and Discussion

3.1. Structural Properties

Structural properties have a significant impact on how materials behave, function, perform, and how they are processed in a variety of settings. Thus, in order to advance technology, innovation, and scientific knowledge across a wide range of sectors, it is imperative to comprehend and manage the structures of materials [21]. Figure 2 shows the total energy against the normalized unit cell volumes for both materials. The lattice parameters shown in Table 1 were obtained from the lowest points of Figure 2.

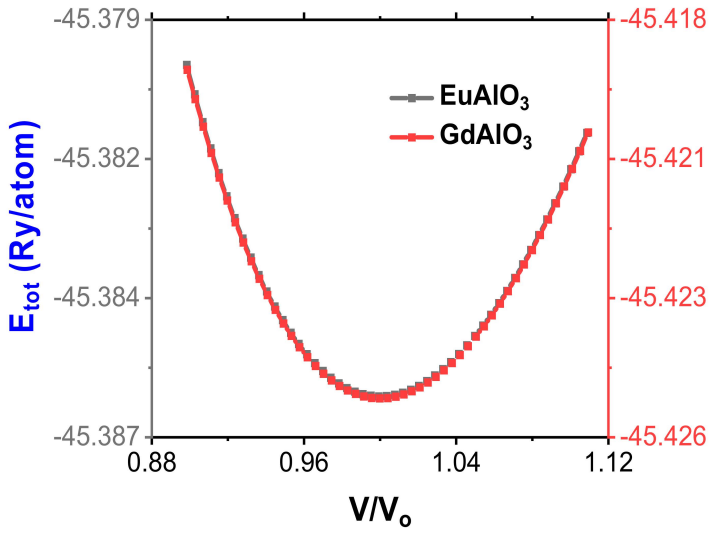


Figure 2. Total energy per atom against unit cell volumes for both $EuAlO_3$ and $GdAlO_3$.

It is evident that both materials contracted after optimization, since the lattice parameters shown in Table 1 are slightly lower than the reference values [15,16]. However, they are very close to those of some previously determined values, both experimentally and computationally, which shows the reliability of the results obtained in this study. The structural stabilities of the two perovskites were determined by calculating their formation energies, which are also presented in Table 1. The negative values of the formation energies show that both materials are structurally stable. However, $GdAlO_3$ is slightly more structurally stable than $EuAlO_3$, as it has a lower formation energy. This is in line with their total energies, as depicted in Figure 2. Structural stability is critical for the performance, efficiency, and longevity of materials used in optoelectronic devices. Any notable alteration or deterioration in the material's structure can have an immediate effect on the functionality of these devices, because they depend on specific electrical and optical properties. Thus, $GdAlO_3$ is better than $EuAlO_3$ in this regard. Materials having particular band gaps, carrier mobilities, and optical absorption/emission properties are essential for optoelectronic devices like LEDs and photodetectors; and are guaranteed to hold true always, and in a variety of operating environments, including those involving temperature and mechanical stress, thanks to their structural stability. Furthermore, a variety of temperatures are frequently used by optoelectronic devices, occasionally rising as a result of electrical currents or external environmental factors. Thus, structural stability guarantees that at higher temperatures, these materials will retain their chemical makeup and crystalline structure [22]. Thus, in terms of structural stabilities, $GdAlO_3$ is superior to $EuAlO_3$.

Table 1. The calculated structural properties of the two materials ($EuAlO_3$ and $GdAlO_3$) at the ground state.

Parameter	a (Å)	ρ (kg/m^3)	H_f (eV/atom)
$EuAlO_3$	3.728 (3.69–3.72 [23]) (3.72 [24])	7273 (7010 [25])	−3.779
$GdAlO_3$	3.719 (3.71 [26,27])	7492	−3.782 (−3.18 [26])

The mechanical stability, temperature control, performance, and manufacturability of devices such as LEDs, lasers, and photodetectors are all impacted by a material's density, which is a significant factor that determines its suitability for optoelectronic applications. The practical applications of optoelectronic materials can be impacted by their density in a number of ways; in that for those devices that need to be portable, flexible, or integrated into lightweight systems, low–density materials are beneficial. High–density materials frequently exhibit superior thermal conductivity, which is necessary for effective heat dissipation in high–power devices like high-power transistors, laser diodes, and LEDs. With a density of 4.0 g/cm^3, sapphire—a common substrate for LEDs and laser diodes—contributes to its mechanical strength and longevity. With a density of 6.15 g/cm^3, gallium nitride (a material that is also frequently used in high-power LEDs and lasers) offers good mechanical and thermal stability [28]. Therefore, the optoelectronic industry may find both the two materials investigated in this study valuable.

3.2. Mechanical Properties

Although optical and electronic performance are the main criteria used to evaluate optoelectronic devices, their mechanical properties are equally crucial to their dependability, flexibility, durability, and manufacturing feasibility. Mechanical properties are highly relevant for materials used in optoelectronic devices. While these devices are primarily evaluated based on their optical and electronic performance, their mechanical properties play a significant role in their durability, flexibility, manufacturability, and reliability. Figure 3 shows four elastic constants, which are all observed to decrease with an increase in temperature. This is a general trend that is observed in most materials, and is attributed to the thermal expansion effects, as well

as changes in the atomic or molecular structure. However, the decrease in elastic constants with an increase in temperature indicates reduced mechanical stability of both materials at higher temperatures. This may result in increased susceptibility to deformation, yielding, or failure under applied stress.

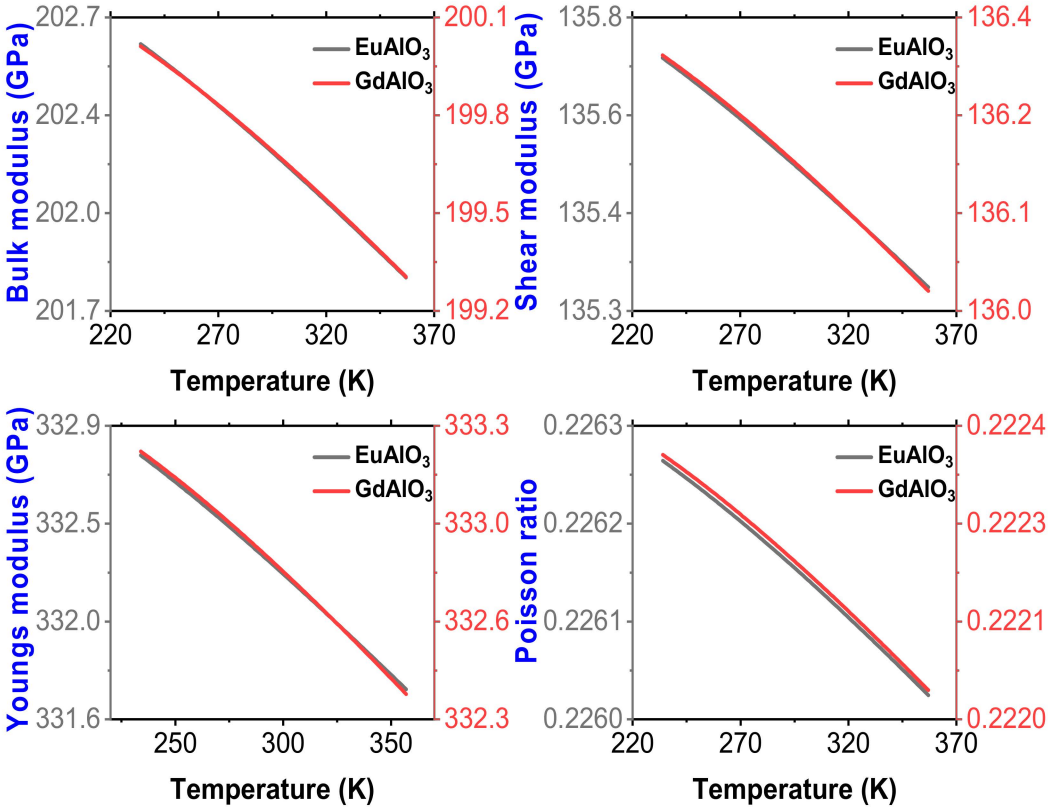


Figure 3. Elastic constants of $EuAlO_3$ and $GdAlO_3$ as functions of temperature.

The mechanical stability of materials also plays a critical role in both the fabrication and performance of optoelectronic device in that materials with poor mechanical stability may develop cracks, voids, or delamination under residual or thermal stresses. Moreover, it leads to uneven film thickness, affecting the mechanical properties. In miniaturized and flexible optoelectronic devices such as wearable sensors or flexible displays, mechanical stability is even more critical. Materials must thus withstand bending, stretching, and compression without losing functionality.

Mechanical stresses can impact the electrical performance of optoelectronic devices by altering their electronic properties or inducing microstructural defects. A decrease in elastic constants with temperature may affect the material's ability to maintain proper contact between layers or interfaces within the device, leading to increased series resistance, or reduced charge carrier mobility. The computed mechanical properties of both materials (Table 2) show a very good agreement with those found in the literature, which confirms the reliability of the results. Although DFT has a number of limitations, most of them, such as band gap underestimation and inadequate description of magnetic systems, were not investigated in this study. Moreover, the calculations were performed in a range of temperatures, which limits the inaccuracies that may arise from the ground–state calculations. A closer look at the percentage change in the elastic constants of the two materials (Table 2) reveals that $EuAlO_3$ suffers more change in the elastic constants. Thus, $GdAlO_3$ turns out to outperform $EuAlO_3$ in this regard, although with a very narrow margin. This is crucial for optoelectronic devices such as lasers, photodetectors, and modulators, where mechanical strain can lead to changes in the refractive index and birefringence of the material. A smaller change in elastic constants thus ensures that these optical properties remain stable

under mechanical stress or external influences. Moreover, devices such as LEDs and laser diodes rely on precise control of electronic and optical properties and therefore, stability in elastic constants minimizes strain–induced distortions, ensuring consistent performance, such as emission wavelength and efficiency [29].

Table 2. The computed room temperature properties of $EuAlO_3$ and $GdAlO_3$. μ is the Poisson ratio, while σ is the thermal stress. a is in Å, B, G, E, and σ are in GPa, while γ is in K^{-1}.

Material.		B	G	E	M	γ ($\times 10^{-6}$)	σ
$EuAlO_3$	Max	202.63	135.68	332.77	0.2263	8.4987	−0.01715
	Min	201.82	135.29	331.74	0.2260	6.5856	−0.01334
	% change	0.4013	0.2883	0.3105	0.1327	29.050	28.561
	Room	202.22 197.34 [14]	135.48 131.90 [14]	332.25 323.60 [14]	0.2262 0.226 [14]	7.9471	−0.01607
$GdAlO_3$	Max	200.01	136.30	333.21	0.2223	6.7719	−0.0135
	Min	199.30	136.00	332.40	0.2220	4.7180	−0.00944
	% change	0.3562	0.2206	0.2437	0.1351	43.532	43.008
	Room	199.66 209.87 [23]	136.15 143.93 [23]	332.81 351.45 [23]	0.2222 0.30 [23]	6.1015	−0.01218

For materials used in optoelectronic applications, a larger bulk modulus is important because it indicates the material's resistance to compression, which has a direct impact on the mechanical resilience, longevity, and performance of the device in a number of ways. A material's bulk modulus, which expresses how incompressible it is under uniform pressure, is a vital indicator of its structural integrity and performance stability under environmental and operational loads. Moreover, many optoelectronic devices, particularly high–power LEDs and laser diodes, generate heat during operation. A material with a higher bulk modulus is therefore typically more resistant to thermal-induced deformation, which can help in maintaining the structural integrity of the device at high operating temperatures. Most of the materials that have been investigated for optoelectronic application, including SnSe and SnS, show very low values of the bulk modulus of 60 GPa and below. Thus, although $EuAlO_3$, which has a slightly higher bulk modulus (Figure 3 and Table 2) is better than $GdAlO_3$, both are far much better than most of the materials that have been investigated for the optoelectronic application [30].

In the optoelectronic field, a higher shear modulus is significant because it directly influences the mechanical robustness, stability, and durability of the materials, which are critical for the long-term performance and reliability of devices like LEDs, lasers, and photodetectors. For instance, materials in LEDs may experience shear stress during bending, thermal expansion, or when mounted in mechanically stressful environments. A high shear modulus reduces the risk of warping, cracking, or layer separation [30]. Figure 3 and Table 2 show that the bulk modulus of $GdAlO_3$ is slightly higher than that of $EuAlO_3$, which indicates that it is better than $EuAlO_3$ in this regard, although both materials possess relatively high values of the shear modulus, which is good for several optoelectronic application, including high-power LEDs, microelectromechanical systems, and laser dioses.

For a number of reasons, a larger Young's modulus is important for optoelectronic applications as it represents a material's resistance to deformation under applied stress. This is especially the case in relation to the mechanical performance, stability, and dependability of materials used in devices like LEDs, lasers, and photodetectors. Resistance to deformation under applied stress is vital for preserving the devices' structural integrity, particularly in high–stress settings when failures may be avoided only by mechanical stability. Furthermore, materials with a large Young's modulus are resistant to deformation from external mechanical forces. This resistance is essential for avoiding delamination or microcracks, which might impair the devices' lifetime and functionality [31].

Both materials have significantly larger Young's moduli than the majority of materials that have been studied for application in the optoelectronic sector, such as GaS, GaSe, GaTe, Sr_2LaNbO_6, and Sr_2LuNbO_6, according to the calculated Young's moduli shown in Figure 3 and Table 2 [31,32]. Nonetheless, it was found that the Young's modulus of $GdAlO_3$ was somewhat greater, indicating that these materials are suitable for the manufacture of photonic integrated circuits, thin–film transistors, and high–power LEDs. In comparison to its axial deformation, a material with a higher Poisson ratio shows more lateral expansion or contraction. A greater Poisson ratio in optoelectronic applications can enhance the coupling between mechanical and optical responses, which is essential for improving the performance and sensitivity of devices that depend on both optical signals and mechanical deformation, such as optomechanical sensors and microelectromechanical systems. Furthermore, dimensional stability under mechanical and thermal stresses can be preserved with a larger Poisson ratio, avoiding problems that might impair device performance, such as layer separation [33]. Thin–film transistors and organic light–emitting diodes are two examples of optoelectronic devices that benefit from this. $EuAlO_3$ has a greater Poisson ratio than $GdAlO_3$, so it is superior.

Ductility is critical during the fabrication of optoelectronic devices, especially for processes that involve thin films, wires, or flexible substrates. Highly ductile materials can be drawn into thin wires or formed into thin films without cracking, which is essential for applications such as interconnects and flexible electronics, where ductile metals like gold and copper are often used for electrical connections in optoelectronic devices because they can be drawn into fine wires or contacts without breaking. Moreover, ductile materials can absorb thermal stresses that arise due to differences in the thermal expansion of different layers or materials in an optoelectronic device. Under heating or cooling, ductile materials can deform slightly, relieving stress and preventing cracking or delamination in rigid or brittle layers. The two materials are not good for the mentioned applications, as they are brittle. Brittle materials have Poisson ratios of less than 0.27, while ductile materials have values of above 0.27 [34,35].

3.3. Thermal Properties

One of the crucial factors affecting the performance and design of materials used in optoelectronic applications is the thermal expansion coefficient (CTE), which gauges how much a substance expands or contracts in response to temperature variations. Figure 4 shows the change in the CTE of both materials with temperature. Optoelectronic devices often rely on precise alignment of components such as lenses, waveguides, and mirrors. Changes in temperature can lead to thermal expansion or contraction, which in turn, can misalign these critical components. A mismatch in CTE between different materials can also cause the misalignment to worsen, which affects light transmission efficiency, wavelength shift, signal integrity in optical fibers, and even the refractive index variations. Thus, for applications requiring high precision, such as photonic integrated circuits or laser systems, materials with compatible CTEs are essential in order to maintain alignment and optical performance. A number of the optoelectronic devices are fabricated on sapphire glass, which has a CTE of 5.312–9.317 $\times$ 10^{-6} K^{-1} [36]. These values are quite within the range of the computed values in this study (Table 2). Both materials are therefore ideal for manufacture of LEDs, laser diodes, and high electron-mobility transistors. However, as these devices require thermally stable substrates, $EuAlO_3$ proves to be a better alternative compared to $GdAlO_3$, because it suffers less change in the CTE (Table 2).

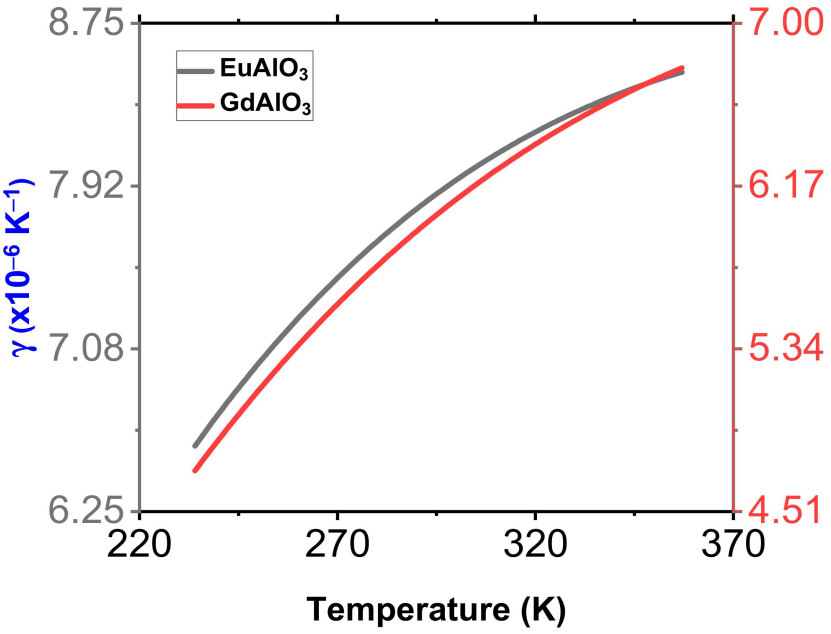


Figure 4. Thermal expansion coefficients of $EuAlO_3$ and $GdAlO_3$ as a function of temperature.

The thermal stability of materials is critical in the fabrication and performance of optoelectronic devices because these devices often operate in environments with varying temperatures and undergo thermal processes during manufacturing. Many fabrication techniques, such as epitaxial growth, annealing, and sintering require materials to withstand high temperatures without degrading or undergoing undesirable changes. As such, materials with poor thermal stability may break down or lose essential properties. Moreover, thermal instability can cause the diffusion of atoms across material interfaces, leading to interfacial defects such as degraded layer quality in heterostructures and altered electronic and optical properties [37].

Thermal stress is the mechanical stress or strain that occurs in a material due to changes in temperature. Figure 5 depicts a decrease in thermal stress for both materials as temperature increases. This is significant, since it indicates improved material performance, structural integrity, manufacturing efficiency, and long-term reliability across a wide range of applications. Thermal stress arises when materials with different CTEs expand or contract at different rates under temperature changes. This can lead to stress at interfaces between different materials, such as between a semiconductor and its substrate, or between various encapsulating materials. A decrease in thermal stress with increasing temperature means that the material is less likely to experience fracture, delamination, or cracking as it heats up, which is critical in devices operating at elevated temperatures, such as high–power LEDs or laser diodes [38].

A lower thermal stress, as exhibited by $GdAlO_3$ (Figure 5 and Table 2), is generally better for optoelectronic devices, as it directly enhances their performance, reliability, and longevity. Moreover, a lower thermal stress means there is less risk of mechanical failures like cracking, delamination, or fracturing at the material interfaces, which could otherwise cause device failure or degradation. Since a smaller change in the thermal stress with temperature is ideal for the optoelectronic device applications, it implies that $EuAlO_3$ is less likely to experience cracking, warping, or delamination. This enhances the reliability of the optoelectronic devices made from $EuAlO_3$, and ensuring consistent performance over time compared to those made from $GdAlO_3$. Moreover, optoelectronic devices manufactured using $GdAlO_3$ with a lower thermal stress can maintain their structural integrity and electrical performance over a longer period, thus extending their lifespan and maximizing their return on investment. However, there is no record about thermal stress of the two materials in the literature, so the data obtained here can be used for future reference [38,39].

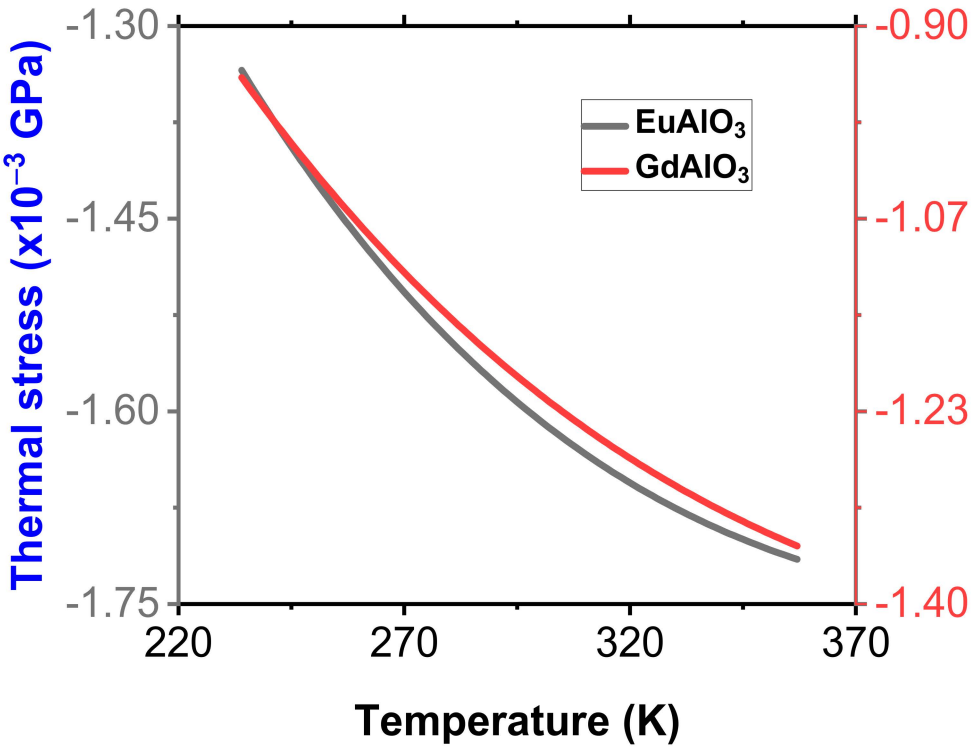


Figure 5. Thermal stress of $EuAlO_3$ and $GdAlO_3$ as a function of temperature.

4. Conclusions

The study successfully compared the thermal properties of $EuAlO_3$ and $GdAlO_3$. The results showed that both materials are structurally stable, although $GdAlO_3$ is more structurally stable compared to $EuAlO_3$, since it has a lower value of the formation energy. This is good for LEDs and photodetectors. The values of the lattice parameters and densities are consistent with those from previous studies. Both materials proved to be heavy, which is good for most optoelectronic applications. The elastic constants of both materials reduced with increase in temperature, implying reduced thermal stability. However, $GdAlO_3$ suffered a smaller change in the elastic constants with temperature. While $GdAlO_3$ recorded higher values of the shear and Young's moduli, $EuAlO_3$ recorded higher bulk modulus and the Poisson ratio. The lower values of the Poisson ratio showed that both materials are brittle. The thermal expansion coefficients of both materials increased with increase in temperature, and could be attributed to increase in the kinetic energies of the particles within the materials as they gain heat. $EuAlO_3$ had a higher value of the volume expansion coefficient, which is close to that of sapphire glass that is commonly used as a substrate in most optoelectronic devices. It also turned out to be more thermally stable than $GdAlO_3$, implying that it can withstand temperature fluctuations without serious degradation better than $GdAlO_3$. The calculated thermal stress of both materials decreased with increase in temperature (which is good for improved performance and structural integrity). $EuAlO_3$ was found to be better at this, as it had a lower thermal stress. Moreover, $EuAlO_3$ was found to suffer much less thermal stress compared to $GdAlO_3$. Although the computed thermal properties of $EuAlO_3$ and $GdAlO_3$ obtained in this study are promising for application in the optoelectronic devices, an experimental verification of the computed mechanical and thermal properties needs to be done. Moreover, the study did not explore the thermal conductivities of the materials, an area that can also be explored.

Author Contributions: Conceptualization, A.B.A.; methodology, A.B.A. and N.O.O.; software, A.B.A. and N.O.O.; validation, A.B.A.; formal analysis, A.B.A. and N.O.O.; investigation, A.B.A.; resources, A.B.A. and N.O.O.; data curation, A.B.A.; writing—original draft preparation, A.B.A. and N.O.O.;

writing—review and editing, A.B.A.; visualization, A.B.A. All authors have read and agreed to the published version of the manuscript.

Funding: This project was funded by the Deanship of Scientific Research (DSR) at King Abdulaziz University, Jeddah, under grant no. (GPIP:1154-130-2024). The authors, therefore, acknowledge with thanks DSR for technical and financial support.

Data Availability Statement: Data is contained within the article.

Conflicts of Interest: The authors declare no conflicts of interest.

References

1. Alruqi, A.B.; Ongwen, N.O. First principles investigation of elastic, electronic and thermoelectric properties of lead-free Cs–X–I (X = Pb, Gd, Nd, Y) perovskites. *J. Phys. Commun.* **2024**. [CrossRef]
2. Das, S.; Gholipour, S.; Saliba, M. Perovskites for laser and detector applications. *Energy Environ. Mater.* **2019**, *2*, 146–153. [CrossRef]
3. Assirey, E. Perovskite synthesis, properties and their related biochemical and industrial application. *Saudi Pharm. J. SPJ* **2019**, *27*, 817–829. [CrossRef]
4. Yang, G.; Bai, S.; Li, X.; Liang, H.; Li, C.; Sun, J.; Wang, Y.; Huang, J.; Pan, G.; Zhu, Y. Tunable and efficient photoluminescence of lanthanide-doped $Cs_2NaScCl_6$ double perovskite single crystals toward multifunctional light-emitting diode applications. *ACS Appl. Mater. Interfaces* **2023**, *15*, 24629–24637. [CrossRef]
5. Zhydachevskyy, Y.; Hizhnyi, Y.; Nedilko, S.; Kudryavtseva, I.; Pankratov, V.; Stasiv, V.; Vasylechko, L.; Sugak, D.; Lushchik, A.; Berkowski, M.; et al. Band gap engineering and trap depths of intrinsic point defects in $RAlO_3$ (R = Y, La, Gd, Yb, Lu) perovskites. *J. Phys. Chemistry. C Nanomater. Interfaces* **2021**, *125*, 26698–26710. [CrossRef]
6. Mattoni, A.; Caddeo, C. Dielectric function of hybrid perovskites at finite temperature investigated by classical molecular dynamics. *J. Chem. Phys.* **2020**, *152*, 104705. [CrossRef]
7. Usman, T.; Khan, S.A.; Khan, S.; Ilyas, A.; Liaqat, K.; Hanif, M. First-principles study of structural, electronic, optical and thermoelectric properties of rare earth-based perovskites $XAlO_3$ (X = Sm, Eu, Gd). *Comput. Theor. Chem.* **2024**, *1235*, 114567. [CrossRef]
8. Mir, W.; Sheikh, T.; Arfin, H.; Xia, Z.; Nag, A. Lanthanide doping in metal halide perovskite nanocrystals: Spectral shifting, quantum cutting and optoelectronic applications. *NPG Asia Mater.* **2020**, *12*, 1–9. [CrossRef]
9. Liu, X.; Li, R.; Xu, X.; Jiang, Y.; Zhu, W.; Yao, Y.; Li, F.; Tao, X.; Liu, S.; Huang, W.; et al. Lanthanide (III)-Cu4I4 organic framework scintillators sensitized by cluster-based antenna for high-resolution X-ray imaging. *Adv. Mater.* **2022**, *35*, 2206741. [CrossRef]
10. Shankar, A.; Rai, D.; Ghimire, M.; Thapa, R. Study of the electronic and magnetic properties of $EuAlO_3$ using FP-LAPW method. *AIP Conf. Proceeding* **2015**, *1661*, 070012. [CrossRef]
11. Rai, D.; Shankar, A.; Ghimire, M.; Khenata, R.; Thapa, R. Study of electronic and magnetic properties in 4f electron based cubic $EuAlO_3$: A first-principles calculation. *Phys. Scr.* **2015**, *90*, 065803. [CrossRef]
12. Abdelkder, B.; Karima, B.; Nabil, B.; Kada, B.; Samir, B. Structural and optoelectronic properties of cubic perovskite type $XAlO_3$ (X = Gd and Dy) theoretical investigation. *Ann. West Univ. Timis. -Phys.* **2023**, *65*, 144–159. [CrossRef]
13. Fabrichnaya, O.; Saenko, I.; Kriegel, M.; Seidel, J.; Zienert, T.; Savinykh, G.; Schreiber, G. Experimental investigation of phase relations and thermodynamic properties in the system ZrO_2-Eu_2O_3-Al_2O_3. *J. Eur. Ceram. Soc.* **2016**, *36*, 1455–1468. [CrossRef]
14. Oudrane, D.; Bourachid, I.; Bouafia, H.; Sahli, B.; Abidri, B.; Rached, D. Computational insights in predicting structural, mechanical, electronic, magnetic and optical properties of $EuAlO_3$ cubic-perovskite using FP-LAPW method. *Comput. Condens. Matter* **2021**, *26*, e00537. [CrossRef]
15. Available online: https://legacy.materialsproject.org/materials/mp-973892/ (accessed on 18 November 2024).
16. Available online: https://legacy.materialsproject.org/materials/mp-1178268/ (accessed on 18 November 2024).
17. Giannozzi, P.; Andreussi, O.; Brumme, T.; Bunau, O.; Nardelli, M.B.; Calandra, M.; Baroni, S. Advanced capabilities for materials modelling with Quantum ESPRESSO. *J. Phys. Condens. Matter* **2017**, *29*, 465901. [CrossRef]
18. Emery, A.; Wolverton, C. High-throughput DFT calculations of formation energy, stability and oxygen vacancy formation energy of ABO_3 perovskites. *Sci. Data* **2017**, *4*, 170153. [CrossRef] [PubMed]
19. Ongwen, N.O.; Ogam, E.; Otunga, H.O. Ab initio study of elastic properties of orthorhombic cadmium stannate as a substrate for the manufacture of MEMS devices. *Mater. Today Commun.* **2021**, *26*, 101822. [CrossRef]
20. Thakur, B.; Gong, X.; Dal Corso, A. Ab initio thermodynamic properties of iridium: A high-pressure and high-temperature study. *Comput. Mater. Sci.* **2024**, *234*, 112797. [CrossRef]
21. Leszek, W. On the significance of structure-property relationships. *Terotechnology* **2018**, *5*, 41–46. [CrossRef]
22. Li, X.; Tao, L.; Chen, Z.; Fang, H.; Li, X.; Wang, X.; Xu, J.; Zhu, H. Graphene and related two-dimensional materials: Structure-property relationships for electronics and optoelectronics. *Appl. Phys. Rev.* **2017**, *4*, 021306. [CrossRef]
23. Usman, T.; Murtaza, G.; Luo, H.; Mahmood, A. GGA and GGA + U study of rare earth-based perovskites in cubic phase. *J. Supercond. Nov. Magn.* **2017**, *30*, 1389–1396. [CrossRef]
24. Verma, A.S.; Jindal, V.K. Lattice constant of cubic perovskites. *J. Alloys Compd.* **2009**, *485*, 514–518. [CrossRef]

25. Petrov, D.; Angelov, B.; Lovchinov, V. Magnetic susceptibility and surface properties of $EuAlO_3$ nanocrystals. *J. Alloys Compd.* **2011**, *509*, 5038–5041. [CrossRef]
26. Butt, M.K.; Yaseen, M.; Bhatti, I.A.; Iqbal, J.; Murtaza, A.; Iqbal, M.; Laref, A. A DFT study of structural, magnetic, elastic and optoelectronic properties of lanthanide based $XAlO_3$ (X = Nd, Gd) compounds. *J. Mater. Res. Technol.* **2020**, *9*, 16488–16496. [CrossRef]
27. Jiang, L.Q.; Guo, J.K.; Liu, H.B.; Zhu, M.; Zhou, X.; Wu, P.; Li, C.H. Prediction of lattice constant in cubic perovskites. *J. Phys. Chem. Solids* **2006**, *67*, 1531–1536. [CrossRef]
28. Moody, G.; Islam, M. Materials for ultra-efficient, high-speed optoelectronics. *MRS Bull.* **2022**, *47*, 475–484. [CrossRef]
29. Gagui, S.; Ghemid, S.; Meradji, H.; Zaidi, B.; Tahir, S.; Ahmed, R.; Kushwaha, A.; Hadjoudja, B.; Chouial, B. Tailoring of elastic, optoelectronic, and thermal properties of antimony doped indium phosphorus alloys for optoelectronic applications. *J. Alloys Compd.* **2020**, *858*, 157632. [CrossRef]
30. Sarkar, A.S.; Konidakis, I.; Gagaoudakis, E.; Maragkakis, G.M.; Psilodimitrakopoulos, S.; Katerinopoulou, D.; Stratakis, E. Liquid phase isolation of SnS monolayers with enhanced optoelectronic properties. *Adv. Sci.* **2022**, *10*, 2201842. [CrossRef]
31. Cui, Y.; Li, S.; Zhang, X.; Wang, T.; Cao, X.; Yan, S.; Zhang, X.; Lei, H.; Tang, G.; Hong, J.; et al. In-plane anisotropic mechanical properties of two-dimensional $NbOI_2$. *Appl. Phys. Lett.* **2023**, *123*, 051905. [CrossRef]
32. Hanif, A.; Aldaghfag, S.; Aziz, A.; Yaseen, M.; Murtaza, A. Theoretical investigation of physical properties of Sr_2XNbO_6 (X = La, Lu) double perovskite oxides for optoelectronic and thermoelectric applications. *Int. J. Energy Res.* **2022**, *46*, 10633–10643. [CrossRef]
33. Bai, L.; Gao, Y.; Peng, J.; Xie, X.; Wen, M.; Dong, H.; Zhang, X.; Huang, L.; Wu, F. Zero Poisson's ratio in single-layer arsenic. *Nanoscale* **2022**, *14*, 969–975. [CrossRef] [PubMed]
34. Ongwen, N.O.; Ogam, E.; Fellah, Z.E.A.; Mageto, M.; Othieno, H.; Otunga, H. Thermal properties and pressure-dependent elastic constants of cadmium stannate as a substrate for MEMS: An ab initio study. *Phys. B Condens. Matter* **2023**, *651*, 414599. [CrossRef]
35. Ongwen, N. Synthesis and characterization of cadmium tin oxide for MEMS substrates and its comparative computational study with silicon and silicon carbide. *Braz. J. Phys.* **2024**, *54*, 254. [CrossRef]
36. Döhler, F.; Zscheckel, T.; Kasch, S.; Schmidt, T.; Rüssel, C. A glass in the $CaO/MgO/Al_2O_3/SiO_2$ system for the rapid laser sealing of alumina. *Ceram. Int.* **2017**, *43*, 4302–4308. [CrossRef]
37. Zhao, C.; Hurtado, L.; Javey, A. Thermal stability for Te-based devices. *Appl. Phys. Lett.* **2020**, *117*, 192104. [CrossRef]
38. Oriach-Font, C.; Carbonell-Sanromà, E.; Safont-Camprubí, G.; Tricas-Mendoza, S.; Garcia-Cubero, C. Effect of stress on the temperature coefficient of solder-free mounted laser diode bars. In *Components and Packaging for Laser Systems VIII.*; SPIE: St Bellingham, WA, USA, 2022; Volume 11982, pp. 50–56. [CrossRef]
39. Mezzalira, C.; Conti, F.; Pedron, D.; Signorini, R. Thermomechanical stresses in silicon chips for optoelectronic devices. *Appl. Sci.* **2023**, *13*, 2737. [CrossRef]

Disclaimer/Publisher's Note: The statements, opinions and data contained in all publications are solely those of the individual author(s) and contributor(s) and not of MDPI and/or the editor(s). MDPI and/or the editor(s) disclaim responsibility for any injury to people or property resulting from any ideas, methods, instructions or products referred to in the content.